PHYSICAL REVIEW B **73**, 220407(R) (2006)

Scaling of terahertz conductivity at the metal-insulator transition in doped manganites

A. Pimenov,[1] M. Biberacher,[1] D. Ivannikov,[1] A. Loidl,[1] A. A. Mukhin,[1,2] Yu. G. Goncharov,[2] and A. M. Balbashov[3]
[1]*Experimentalphysik V, Center for Electronic Correlations and Magnetism, Universität Augsburg, 86135 Augsburg, Germany*
[2]*General Physics Institute of the Russian Academy of Sciences, 119991 Moscow, Russia*
[3]*Moscow Power Engineering Institute, 105835 Moscow, Russia*
(Received 30 January 2006; published 26 June 2006)

Magnetic field and temperature dependence of the terahertz conductivity and permittivity of the colossal magnetoresistance manganite $Pr_{0.65}Ca_{0.28}Sr_{0.07}MnO_3$ (PCSMO) is investigated approaching the metal-to-insulator transition (MIT) from the insulating side. In the charge-ordered state of PCSMO both conductivity and dielectric permittivity increase as a function of magnetic field and temperature. Universal scaling relationships $\Delta\varepsilon \propto \Delta\sigma$ are observed in a broad range of temperatures and magnetic fields. Similar scaling is also seen in $La_{1-x}Sr_xMnO_3$ for different doping levels. The observed proportionality points towards the importance of pure ac-conductivity and phononic energy scale at MIT in manganites.

DOI: 10.1103/PhysRevB.73.220407 PACS number(s): 75.47.Gk, 71.30.+h, 72.20.Ee, 77.22.Ch

Physical properties of doped manganites are governed by a complex interplay of charge, lattice, orbital, and spin degrees of freedom, which lead to a large variety of unusual effects.[1] While known since early works by Jonker and van Santen[2] and Wollan and Koehler[3] the interest in these compounds was enormously stimulated by the observation of large magnetoresistance effects in thin manganite films.[4] It is generally accepted now[5] that the magnetoresistance effects in manganites are strongly influenced by electronic phase separation[6] between paramagnetic or antiferromagnetic (AFM) insulating and ferromagnetic (FM) metallic regions which coexist on a microscopic scale close to the metal-to-insulator transition (MIT).

Particularly large values of magnetoresistance have been observed[7] in Ca-doped $PrMnO_3$ (PCMO),[8] which has been explained as a consequence of the first-order transition[9,10] between charge- and orbitally ordered insulating[11] and ferromagnetic metallic phases.[12] Although phase-separation effects are still important in PCMO,[5,13–16] in order to fully understand the MIT on the basis of electronic phase separation a modification of the standard approach is necessary.[17,18] Additional fine-tuning of PCMO by the substituition of Ca^{2+} by Sr^{2+} (Ref. 19) leads to eleven orders-of-magnitude changes in resistivity in magnetic field.[20,21] The subtle balance of various energy scales in $(Pr:Ca:Sr)MnO_3$ results in new physical effects like the switching of the MIT by light, x-ray, or electric field.[22–25]

In this paper we present the results of the dynamic conductivity experiments at THz frequencies on the insulating side of the metal-to-insulator transition. On approaching the transition a linear relationship between conductivity and dielectric permittivity is observed, both using magnetic field and temperature as tuning parameters. This linearity points towards the importance of the characteristic frequency scale of a few THz for the charge dynamics. Closely similar scaling behavior can also be stated in Sr-doped $LaMnO_3$.

Single crystals of $Pr_{0.65}Ca_{0.28}Sr_{0.07}MnO_3$ (PCSMO), which were used in the present experiments, were grown by the floating-zone method with radiation heating.[26] The samples were characterized using various experimental techniques,[21] and the *B-T* phase diagram has been constructed. Crystals with a typical growth direction [100] were cut from the main rod to a thickness of 0.1–1 mm.

On cooling from room temperature, in zero magnetic field PCSMO reveals a structural phase transition at $T_{CO} \simeq 210$ K into the charge-ordered (CO) insulating phase. On further cooling an AFM phase transition is observed at $T_N \simeq 170$ K, and below $T_{irr} \simeq 100$ K strong hysteresis effects in magnetic fields are observed. Without magnetic field the samples remain in the insulating state down to the lowest temperatures. Strong magnetoresistance effects as high as 10^{10} at $T=50$ K are observed below T_{CO}. Typical values of the external magnetic field to switch between CO insulating and FM metallic state are in the range 2–5 T. Detailed discussion of these results is given in Ref. 21. The *B-T* phase diagram for the samples under investigation[21] agrees well with published results.[10,19]

The dynamic conductivity experiments for frequencies $0.1\ \text{THz} < \nu < 1\ \text{THz}$ were carried out in a Mach-Zehnder interferometer,[27,28] which allows the measurements of transmittance and phase shift of a plane-parallel sample. PCSMO samples of different thicknesses have been utilized. To ensure mechanical stability the thinnest sample (~0.1 mm thick) was glued onto a MgO substrate. The electrodynamic properties of the substrate were obtained in a separate experiment. The experimental data for both single-layer and two-layer systems have been analyzed using the Fresnel optical formulas for the complex transmission coefficient.[29] The absolute values of the complex conductivity $\sigma^* = \sigma_1 + i\sigma_2$ and dielectric permittivity $\varepsilon^* = \varepsilon_1 + i\varepsilon_2 = \sigma^*/i\varepsilon_0\omega$ were determined directly from the measured spectra. Here ε_0 and $\omega = 2\pi\nu$ are the permittivity of vacuum and the angular frequency, respectively. The experiments in external magnetic fields were performed in a superconducting split-coil magnet, which allowed transmission experiments in magnetic fields up to 7 T to be carried out. In order to exclude the influence of the Faraday effect,[30] the experiments were carried out in external magnetic fields perpendicular to the propagation of the electromagnetic beam (Voigt geometry).

Figure 1 shows the temperature dependence of the dynamic conductivity (lower panel) and permittivity (upper panel) of PCSMO at terahertz frequencies in zero external magnetic field. The high-frequency properties reveal only a weak temperature dependence below $T_{CO} \simeq 210$ K. The small changes of the conductivity in this temperature range

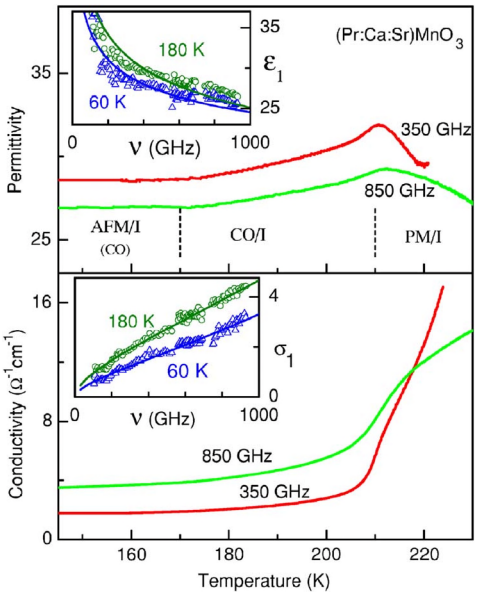

FIG. 1. (Color online) Temperature dependence of the permittivity (upper panel) and conductivity (lower panel) of $Pr_{0.65}Ca_{0.28}Sr_{0.07}MnO_3$ at 350 GHz and 850 GHz. Dashed lines indicate the transition temperature between different phases: PM, paramagnetic; CO, charge ordered; AFM, antiferromagnetic; I, insulator. The insets show the frequency dependencies of conductivity and permittivity in the THz frequency range. Symbols correspond to the experimental data, lines are fits according to Eq. (1) and Ref. 35 using $s=0.8$, $\nu_c=2.4$ THz, $A\nu_c^s=6.3\ \Omega^{-1}\ \mathrm{cm}^{-1}$ (60 K), and $A\nu_c^s=8.4\ \Omega^{-1}\ \mathrm{cm}^{-1}$ (180 K).

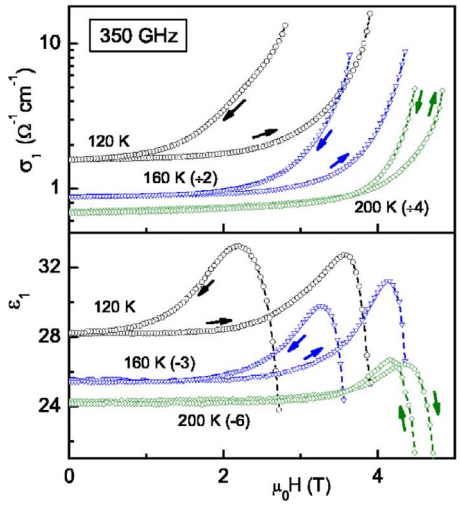

FIG. 2. (Color online) Magnetic field dependence of the permittivity (lower panel) and conductivity (upper panel) of $Pr_{0.65}Ca_{0.28}Sr_{0.07}MnO_3$ at 350 GHz and for different temperatures. The curves were shifted for clarity as indicated in the brackets.

are in marked contrast to the activated behavior of the dc resistivity.[21] This is the consequence of the hopping mechanism of the charge transport and is typical for systems with localization.[31] For these systems it is generally observed that the dc conductivity reveals an exponential temperature dependence, while the temperature dependence of ac conductivity is comparatively weak.[32,33] Approaching $T_{CO}\simeq 210$ K from below, the dynamic conductivity starts to increase rapidly and the permittivity exhibits a cusplike maximum at T_{CO}. Similar to recent results on the MIT in Fe_3O_4 (Ref. 28), the decrease of the permittivity for $T>T_{CO}$ can be ascribed to the growth of a Drude-like contribution of the mobile carriers to the dynamic conductivity, which now is dominated by the dc contribution, while the ac processes become reduced.

The insets in Fig. 1 show the characteristic conductivity and permittivity spectra of PCSMO in the frequency range of our experiment. The conductivity (lower panel) is an increasing function of frequency and follows well the power-law dependence

$$\sigma_1(\nu)=\sigma_{\mathrm{dc}}+\frac{A\nu^s}{1+(\nu/\nu_c)^4}. \qquad (1)$$

Here σ_{dc} is the dc conductivity and s is the power-law exponent. Compared to the conventional expression[34] the additional frequency cutoff ν_c has been introduced in order to preserve the finiteness of the conductivity spectral weight. The application of the Kramers-Kronig transformation to $\sigma(\nu)$ leads to an expression for the frequency dependence of the dielectric permittivity,[28,35] which has been used to fit the spectra in the upper inset of Fig. 1. Comparatively poorer agreement between experimental data and the calculations are due to small relative changes in the dielectric permittivity ($\sim$25% in our frequency range). By investigating PCSMO using broadband dielectric spectroscopy, a superlinear power law has been detected[33] at high frequencies and low temperatures. The downward curvature in $\varepsilon_1(\nu)$ above 800 GHz (upper inset in Fig. 1) probably corresponds to this regime.

Figure 2 shows the magnetic-field-dependence of the conductivity and the dielectric permittivity of PCSMO at $\nu=350$ GHz as a function of the external magnetic field. Starting from $B=0$ and for increasing fields, both the conductivity and permittivity initially increase. The increase of the dielectric permittivity approaching the MIT in doped semiconductors has been investigated earlier and is known as *dielectric catastrophe*.[36] For even higher magnetic fields the increase of the conductivity in PCSMO continues, but the dielectric permittivity starts to decrease. Interestingly, similar behavior is observed in Fig. 1 with temperature as a tuning parameter approaching the MIT. Based on structural data, the temperature range close to the MIT has been identified as a melting of the charge-ordered state in PCSMO.[7,19] In analogy, the upturn in the magnetic-field-dependence of the dielectric permittivity in Fig. 2 is probably due to the melting of the charge-ordered state under the influence of the external magnetic field.

Figure 3 shows the dielectric permittivity of PCSMO replotted as a function of the conductivity. This plot, with the magnetic field as a parameter, allows us to check a possible scaling between conductivity and dielectric permittivity. In this presentation, the zero-field values of σ_1 and ε_1 have been subtracted and only the field-dependent changes are shown. Surprisingly, all data between 60 K and 200 K, i.e., in the charge-ordered state, converge into one universal linear relationship of permittivity and conductivity that is emphasized by the dashed lines in Fig. 3. Solely close to the

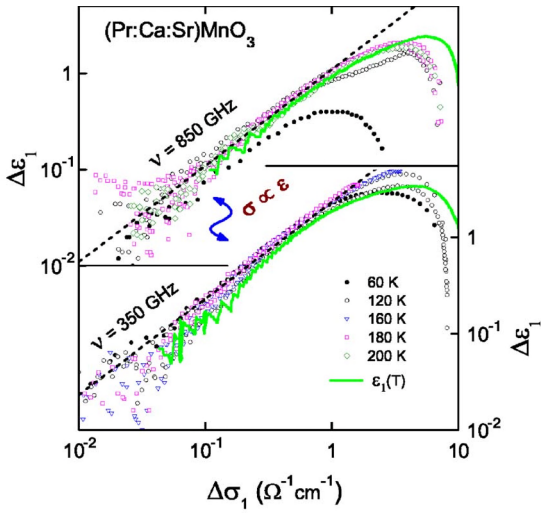

FIG. 3. (Color online) Dielectric permittivity of PCSMO replotted as a function of conductivity at $\nu=350$ GHz (lower panel) and $\nu=850$ GHz (upper panel). The data are shown for fixed temperatures varying the magnetic field (symbols) and for $B=0$ varying the temperature (solid lines). The dashed lines indicate linear scaling between permittivity and conductivity.

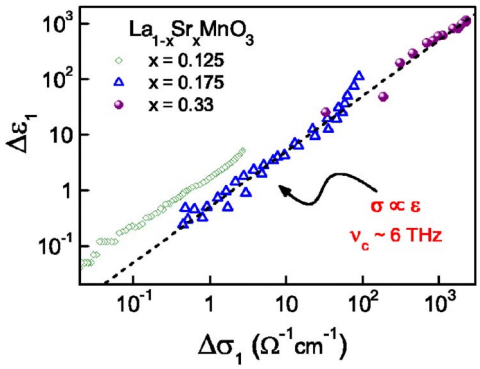

FIG. 4. (Color online) Dielectric permittivity of $La_{1-x}Sr_xMnO_3$ plotted as function of conductivity with the temperature as tuning parameter and for $B=0$. Open diamonds, $x=0.125$ [single crystal (Ref. 41)], open triangles, $x=0.175$ [single crystal (Ref. 41)] closed circles, $x=0.33$ [thin film (Ref. 43)]. The data correspond to the frequency range 400–1000 GHz. The dashed line indicates a linear scaling between permittivity and conductivity.

melting of the CO state this proportionality between conductivity and permittivity breaks down. We note that the same proportionality between σ_1 and ε_1 is observed with the temperature as an explicit parameter. These data correspond to the temperature dependence in Fig. 1 and are shown in the scaling plot (Fig. 3) as a solid line.

An explanation for the scaling $\sigma_1 \propto \varepsilon_1$ can be obtained on the basis of the power law of the conductivity, Eq. (1). Within this model the dielectric permittivity can be proportional to the conductivity neglecting σ_{dc} as well as ε_∞ and assuming fixed power-law exponent s and cutoff frequency ν_c.[35] This constitutes an important result of this work: dielectric constant and conductivity in manganites are dominated solely by ac contributions when approaching the MIT. Taking the power-law exponent $s=0.8$ from the fits in Fig. 1 and using the scaling of Fig. 3, the cutoff frequency can be estimated as $\nu_c \approx 2$ THz, which is in agreement with $\nu_c = 2.4$ THz from the fits in Fig. 1. (We note that changing the value of the power-law exponent s only weakly influences the cutoff frequency.) The cutoff frequency of the insulating state lies in the frequency range of phonons and points towards the phononic mechanism of the hopping conductivity in PCSMO.

At the same time, dc and ac conductivity are closely connected,[31] especially close to MIT. Depending upon the conduction mechanism, this can be due to the hopping mechanism of the conductivity,[37] or reflect different frequency scales in the phase-separation scenario.[5] In the former case the observed cutoff frequency characterizes the maximum hopping rate of charge carriers, which is therefore phonon mediated. Assuming a phase separation, the cutoff characterizes the relaxation within an elementary *RC* circuit between insulating and metallic droplets.

In contrast to recent reports on colossal dielectric constants in manganites[38] the observed high-frequency values are comparatively low. Neither contacts nor internal-barrier layers contributions[39] play a role in THz quasioptic experiments. However, due to the dominating term $\varepsilon_1 \sim (\sigma_1 - \sigma_{dc})/\nu \sim \nu^{s-1}$ (Ref. 35), the permittivity at low frequencies indeed can diverge, and an estimate with the parameters in Fig. 1 leads to the values above $\varepsilon_1 \sim 1000$ at kHz frequencies.

Finally, we compare the observed scaling behavior in PCSMO with the temperature dependence of the conductivity and permittivity in Sr-doped $LaMnO_3$. The parent compound $LaMnO_3$ is an insulator and orders antiferromagnetically below $T_N=140$ K. On substituting La^{3+} by Sr^{2+} (Refs. 40–42) metallic behavior sets in for doping levels above ~16%. Figure 4 shows the parametric dependence of the dielectric permittivity in $La_{1-x}Sr_xMnO_3$ for different doping levels. The data correspond to two metallic compositions, $x=0.175$ (Ref. 41) (single crystals) and $x=0.33$ (Ref. 43) (thin films), and to one composition in the insulating part of the diagram, $x=0.125$ (Ref. 41) (single crystals). In full analogy with the results for PCSMO, the data in Fig. 4 reveal a direct proportionality between conductivity and permittivity. Again, similar arguments allow estimation of the characteristic frequency of the underlying process, $\nu_c \sim 6$ THz. This documents that at high frequencies ($\nu > 300$ GHz) even in the "metallic manganites" the ac conductivity dominates over dc processes.

In conclusion, dynamic conductivity and permittivity of $(Pr:Ca:Sr)MnO_3$ have been investigated close to the magnetic-field-induced metal-to-insulator transition (MIT) and at THz frequencies. Approaching the transition from the insulating side the changes in conductivity and permittivity are directly proportional to each other. Within simple arguments this proportionality indicates that the charge transport close to MIT is governed by ac processes with a characteristic frequency in the phonon range. Closely similar scaling can be observed in Sr-doped $LaMnO_3$ thus suggesting the universality of the MIT in manganites.

The stimulating discussion with P. Lunkenheimer is gratefully acknowledged. This work was supported by BMBF (13N6917/0-EKM) and by DFG (SFB 484).

[1] M. B. Salamon and M. Jaime, Rev. Mod. Phys. **73**, 583 (2001).
[2] G. H. Jonker and J. H. van Santen, Physica (Amsterdam) **16**, 337 (1950); **19**, 120 (1953).
[3] E. O. Wollan and W. C. Koehler, Phys. Rev. **100**, 545 (1955).
[4] K. Chahara, T. Ohno, M. Kasai, and Y. Kozono, Appl. Phys. Lett. **63**, 1990 (1993); R. von Helmolt, J. Wecker, B. Holzapfel, L. Schultz, and K. Samwer, Phys. Rev. Lett. **71**, 2331 (1993); S. Jin, T. H. Tiefel, M. McCormack, R. A. Fastnacht, R. Ramesh, and L. H. Chen, Science **264**, 413 (1994).
[5] E. Dagotto, T. Hotta, and A. Moreo, Phys. Rep. **344**, 1 (2001).
[6] E. L. Nagaev, Sov. Phys. Usp. **39**, 781 (1996).
[7] H. Yoshizawa, H. Kawano, Y. Tomioka, and Y. Tokura, Phys. Rev. B **52**, R13145 (1995); Y. Tomioka, A. Asamitsu, Y. Moritomo, and Y. Tokura, J. Phys. Soc. Jpn. **64**, 3626 (1995).
[8] Z. Jirák, S. Krupička, V. Nekvasil, E. Pollert, G. Villeneuve, and F. Zounová, J. Magn. Magn. Mater. **15-18**, 519 (1980); Z. Jirák, S. Krupička, Z. Šimša, M. Dlouhá, and S. Vratislav, *ibid.* **53**, 153 (1985); E. Pollert, S. Krupička, and E. Kuzmičová, J. Phys. Chem. Solids **43**, 1137 (1982).
[9] V. Hardy, A. Maignan, S. Hébert, and C. Martin, Phys. Rev. B **67**, 024401 (2003).
[10] Y. Tomioka, A. Asamitsu, H. Kuwahara, Y. Moritomo, and Y. Tokura, Phys. Rev. B **53**, R1689 (1996).
[11] M. v. Zimmermann, J. P. Hill, D. Gibbs, M. Blume, D. Casa, B. Keimer, Y. Murakami, Y. Tomioka, and Y. Tokura, Phys. Rev. Lett. **83**, 4872 (1999).
[12] J. A. Fernandez-Baca, Pengcheng Dai, H. Kawano-Furukawa, H. Yoshizawa, E. W. Plummer, S. Katano, Y. Tomioka, and Y. Tokura, Phys. Rev. B **66**, 054434 (2002).
[13] A. Anane, J.-P. Renard, L. Reversat, C. Dupas, P. Veillet, M. Viret, L. Pinsard, and A. Revcolevschi, Phys. Rev. B **59**, 77 (1999).
[14] G. R. Blake, L. Chapon, P. G. Radaelli, D. N. Argyriou, M. J. Gutmann, and J. F. Mitchell, Phys. Rev. B **66**, 144412 (2002).
[15] L. M. Fisher, A. V. Kalinov, I. F. Voloshin, N. A. Babushkina, K. I. Kugel, and D. I. Khomskii, Phys. Rev. B **68**, 174403 (2003).
[16] M. Uehara, S. Mori, C. H. Chen, and S.-W. Cheong, Nature (London) **399**, 560 (1999).
[17] J. Burgy, E. Dagotto, and M. Mayr, Phys. Rev. B **67**, 014410 (2003).
[18] T. Hotta and E. Dagotto, Phys. Rev. B **61**, R11879 (2000).
[19] Y. Tomioka, A. Asamitsu, H. Kuwahara, and Y. Tokura, J. Phys. Soc. Jpn. **66**, 302 (1997); Y. Tomioka and Y. Tokura, Phys. Rev. B **66**, 104416 (2002).
[20] B. Raveau, A. Maignan, and V. Caignaert, J. Solid State Chem. **117**, 424 (1995); A. Maignan, Ch. Simon, V. Caignaert, and B. Raveau, J. Magn. Magn. Mater. **152**, L5 (1996).
[21] J. Sichelschmidt, M. Paraskevopoulos, M. Brando, R. Wehn, D. Ivannikov, F. Mayr, K. Pucher, J. Hemberger, A. Pimenov, H.-A. Krug von Nidda, P. Lunkenheimer, V. Yu. Ivanov, A. A. Mukhin, A. M. Balbashov, and A. Loidl, Eur. Phys. J. B **20**, 7 (2001).
[22] K. Miyano, T. Tanaka, Y. Tomioka, and Y. Tokura, Phys. Rev. Lett. **78**, 4257 (1997).
[23] M. Fiebig, K. Miyano, Y. Tomioka, and Y. Tokura, Science **280**, 1925 (1998).
[24] V. Kiryukhin, D. Casa, J. P. Hill, B. Keimer, A. Vigliante, Y. Tomioka, and Y. Tokura, Nature (London) **386**, 813 (1997).
[25] A. Asamitsu, Y. Tomioka, H. Kuwahara, and Y. Tokura, Nature (London) **388**, 50 (1997).
[26] A. M. Balbashov, S. G. Karabashev, Ya. M. Mukovskii, and S. A. Zverkov, J. Cryst. Growth **167**, 365 (1996).
[27] A. A. Volkov, Yu. G. Goncharov, G. V. Kozlov, S. P. Lebedev, and A. M. Prochorov, Infrared Phys. **25**, 369 (1985).
[28] A. Pimenov, S. Tachos, T. Rudolf, A. Loidl, D. Schrupp, M. Sing, R. Claessen, and V. A. M. Brabers, Phys. Rev. B **72**, 035131 (2005).
[29] M. Born and E. Wolf, *Principles of Optics* (Pergamon, Oxford, 1986).
[30] A. K. Zvezdin and V. A. Kotov, *Modern Magnetooptics and Magnetooptical Materials* (Institute of Physics, Bristol, 1997).
[31] H. Böttger and V. V. Bryksin, *Hopping Conduction in Solids* (VCH, Weinheim, 1985).
[32] A. R. Long, in *Hopping Transport in Solids*, edited by M. Pollak and B. Schklovskii (Elsevier, Amsterdam, 1991), p. 207.
[33] P. Lunkenheimer and A. Loidl, Phys. Rev. Lett. **91**, 207601 (2003).
[34] A. K. Jonscher, *Dielectric Relaxation in Solids* (Chelsea Dielectrics, London, 1983).
[35] Application of the Kramers-Kronig analysis to Eq. (1) gives the following expression for the dielectric constant:

$$\varepsilon_1(\nu) - \varepsilon_\infty = -\frac{\sigma_2(\nu)}{2\pi\nu\varepsilon_0} = \frac{\sigma_1(\nu) - \sigma_{\mathrm{dc}}}{2\pi\nu\varepsilon_0}\left(\tan(s\pi/2) - \frac{(\nu/\nu_c)^{1-s}}{\cos(s\pi/2)}\left\{\sin\left[(s+1)\frac{\pi}{4}\right] + \left(\frac{\nu}{\nu_c}\right)^2 \cos\left[(s+1)\frac{\pi}{4}\right]\right\}\right),$$

where ε_∞ is the high-frequency dielectric constant. This expression is valid both for $s<1$ and for $s>1$.
[36] N. F. Mott, *Metal-Insulator Transitions* (Taylor & Francis, London, 1990), p. 35.
[37] J. P. Dyre and Th. B. Schrøder, Rev. Mod. Phys. **72**, 873 (2000).
[38] N. Biškup, A. de Andrés, J. L. Martinez, and C. Perca, Phys. Rev. B **72**, 024115 (2005); R. S. Freitas, J. F. Mitchell, and P. Schiffer, Phys. Rev. B **72**, 144429 (2005).
[39] P. Lunkenheimer, V. Bobnar, A. V. Pronin, A. I. Ritus, A. A. Volkov, and A. Loidl, Phys. Rev. B **66**, 052105 (2002).
[40] A. Urushibara, Y. Moritomo, T. Arima, A. Asamitsu, G. Kido, and Y. Tokura, Phys. Rev. B **51**, 14103 (1995).
[41] A. Pimenov, C. Hartinger, A. Loidl, A. A. Mukhin, V. Yu. Ivanov, and A. M. Balbashov, Phys. Rev. B **59**, 12419 (1999).
[42] A. Seeger, P. Lunkenheimer, J. Hemberger, A. A. Mukhin, V. Yu. Ivanov, A. M. Balbashov, and A. Loidl, J. Phys.: Condens. Matter **11**, 3273 (1999).
[43] C. Hartinger, A. Pimenov, A. Loidl, and A. M. Balbashov (unpublished).